

Linkage Disequilibrium and Population Structure in Wild and Cultivated Populations of Rubber Tree (*Hevea brasiliensis*)

1 Livia Moura de Souza^{1,¶}, Luciano H. B. dos Santos^{1,¶}, João R. B. F. Rosa^{2,8}, Carla C. da Silva¹,
2 Camila C. Mantello^{1,9}, André R. O. Conson¹, Erivaldo José Scaloppi Junior³, Josefino de
3 Freitas Fialho⁴, Mario Luiz Teixeira de Moraes⁵, Paulo de S. Gonçalves³, Gabriel R. A.
4 Margarido², Antonio A. F. Garcia², Vincent Le Guen⁶, Anete P. de Souza^{1,7,*}

5 ¹ Molecular Biology and Genetic Engineering Center (CBMEG), University of Campinas
6 (UNICAMP), Campinas, SP, Brazil

7 ² Departamento de Genética, Escola Superior de Agricultura “Luiz de Queiroz” Universidade de São
8 Paulo (ESALQ/USP), Piracicaba, SP, Brazil

9 ³ Center of Rubber Tree and Agroforestry Systems, Agronomic Institute (IAC), Votuporanga, SP,
10 Brazil

11 ⁴ Embrapa Cerrados (EMBRAPA), Planaltina, DF, Brasil

12 ⁵ Departamento de Fitotecnia, Faculdade de Engenharia de Ilha Solteira (UNESP) – Universidade
13 Estadual Paulista, Ilha Solteira, SP, Brazil

14 ⁶ Centre de Coopération Internationale en Recherche Agronomique pour le Développement (CIRAD)
15 UMR AGAP, Montpellier, Hérault, France

16 ⁷ Department of Plant Biology, Biology Institute, University of Campinas (UNICAMP) UNICAMP,
17 Campinas, SP, Brazil

18 ⁸ FTS Sementes S.A., Research and Development Center, Ponta Grossa, PR, Brazil

19 ⁹ National Institute of Agricultural Botany (NIAB), Huntingdon Road, Cambridge CB3 0LE, UK

20 [¶]Both authors contributed equally to this work.

21 *** Correspondence:**

22 Corresponding Author: Anete Pereira de Souza
23 anete@unicamp.br

24 **Keywords:** linkage mapping, genetic diversity, population structure, non-random association,
25 genome-wide association study, *Hevea*

26 **Abstract**

27 Among rubber tree species, which belong to the *Hevea* genus of the Euphorbiaceae family, *Hevea*
28 *brasiliensis* (Willd. ex Adr.de Juss.) Muell. Arg. is the main commercial source of natural rubber
29 production worldwide. Knowledge of the population structure and linkage disequilibrium (LD) of
30 this species is essential for the efficient organization and exploitation of genetic resources. Here, we
31 obtained single-nucleotide polymorphisms (SNPs) using a genotyping-by-sequencing (GBS)
32 approach and then employed the SNPs for the following objectives: (i) to identify the positions of
33 SNPs on a genetic map of a segregating mapping population, (ii) to evaluate the population structure of
34 a germplasm collection, and (iii) to detect patterns of LD decay among chromosomes for future
35 genetic association studies in rubber tree. A total of 626 genotypes, including both germplasm
36 accessions (368) and individuals from a genetic mapping population (254), were genotyped. A total

37 of 77,660 and 21,283 SNPs were detected by GBS in the germplasm and mapping populations,
38 respectively. The mapping population, which was previously mapped, was constructed with 1,062
39 markers, among which only 576 SNPs came from GBS, reducing the average interval between two
40 adjacent markers to 4.4 cM. SNPs from GBS genotyping were used for the analysis of genetic
41 structure and LD estimation in the germplasm accessions. Two groups, which largely corresponded
42 to the cultivated and wild populations, were detected using STRUCTURE and via principal
43 coordinate analysis (PCoA). LD analysis, also using the mapped SNPs, revealed that non-random
44 associations varied along chromosomes, with regions of high LD interspersed with regions of low
45 LD. Considering the length of the genetic map (4,693 cM) and the mean LD (0.49 for cultivated and
46 0.02 for wild populations), a large number of evenly spaced SNPs would be needed to perform
47 genome-wide association studies in rubber tree, and the wilder the genotypes used, the more difficult
48 the mapping saturation.

49 1 Introduction

50 *Hevea brasiliensis*, or the rubber tree, is an important crop species that produces a high-quality
51 natural rubber in commercially viable quantity, accounting for more than 98% of the total natural
52 rubber production worldwide (Priyadarshan and Goncalves, 2003). A native species of the Amazon
53 rainforest, *H brasiliensis* is a diploid ($2n=36$, $n=18$), perennial, and cross-pollinated tree species with
54 an estimated haploid genome size of 1.47 Gb (Tang *et al.*, 2016). This species belongs to the
55 *Euphorbiaceae* family, comprising 11 inter-crossable species, of which *H. brasiliensis* is the most
56 economically important (Gonçalves *et al.* 1990). The rubber tree has a heterozygous nature, with a
57 long growing cycle that includes 5 years before latex collection. Like most forest trees, the rubber
58 tree has a long generation time, which explains the slow progress of breeding this species and
59 elucidating the genetic architecture of its complex traits using traditional approaches. Genetic
60 breeding programs are challenged by a low seed yield per pollination (an average of ten seeds
61 obtained for 100 pollinated flowers) and inbreeding depression, making it difficult to develop the
62 appropriate progeny for classical genetic studies (Lespinasse *et al.*, 2000). Hence, relatively little is
63 known about genome-wide models of recombination, allele frequency variation, and linkage
64 disequilibrium (LD) in this important plant.

65 Over the last 15 years, many genetic maps of the rubber tree have been constructed. The first rubber
66 tree marker-based genetic maps were built with restriction fragment length polymorphisms (RFLPs)
67 and amplified fragment length polymorphisms (AFLPs) (Lespinasse *et al.*, 2000), and dense genetic
68 maps were subsequently constructed using simple sequence repeats (SSRs) (Le Guen *et al.*, 2011;
69 Triwitayakorn *et al.*, 2011; Souza *et al.*, 2013). Saturated genetic linkage maps are important for the
70 identification of genomic regions containing major genes and quantitative trait loci (QTLs)
71 controlling agronomic traits, and such maps are important for further breeding programs.

72 In recent years, advances in next-generation sequencing technology (NGS) have lowered the cost of
73 DNA sequencing to the point that genotyping-by-sequencing (GBS) (Elshire *et al.*, 2011) is now
74 feasible for high-diversity, large-genome species, and a genetic map has been developed using the
75 GBS approach (Pootakham *et al.*, 2015). GBS utilizes restriction enzymes to capture a reduced
76 representation of the target genome, and with DNA-barcoded adapters, it is possible to sequence
77 multiple samples in parallel in a single run using an NGS platform. GBS has recently been applied to
78 the large barley (*Hordeum vulgare* L.) and wheat (*Triticum aestivum*) genomes and has been shown
79 to be an effective tool for developing molecular markers for these species (Poland *et al.*, 2012).

80 Evaluation of the molecular diversity encompassed in rubber tree genetic resources is a prerequisite
81 for their efficient exploitation in breeding and the development of conservation strategies of genetic
82 diversity. de Souza *et al.* (2015) analyzed approximately one thousand cultivated rubber tree
83 accessions originating from various geographic areas in a Brazilian germplasm collection. These
84 accessions were genotyped with 13 SSR markers distributed across the chromosomes of the species,
85 and a total of 408 alleles were identified, 319 of which were shared between groups, while 89 alleles
86 were specific to different groups of accessions.

87 LD is the non-random association of alleles at distinct loci in the genome of a sampled population
88 (Weir, 1979) and is the basis for association mapping approaches. LD can be used for many purposes
89 in plant genomics research and has received considerable attention as a tool for the study of marker-
90 trait associations due to physical linkage, followed by marker-assisted selection (MAS). Another
91 important application of LD is the study of genetic diversity in natural populations and germplasm
92 collections, where it can be employed for the evaluation of population genetics and in crop
93 improvement programs, respectively (Gupta *et al.*, 2005).

94 With the rise of sequence-based genotyping, precise and accurate estimates of population structure
95 and the LD across the genome are now attainable for the rubber tree. Our goals in this study were to
96 characterize the genome distribution of single-nucleotide polymorphisms (SNPs) in a rubber tree
97 mapping population using GBS technology, to examine population structure, to investigate how LD
98 breakdown relates to chromosomes, and to compare the LD between cultivated and wild populations.
99 For this study, we used accessions selected from the germplasm collection previously analyzed by de
100 Souza *et al.* (2015) and a mapping population (PR255 x PB217) previously saturated with SSR
101 markers described by Souza *et al.* (2013) and Rosa *et al.* (submitted).

102 2 Material and methods

103 2.1 Plant materials and DNA extraction

104 Two sets of samples were selected for this study, and a total of 626 samples were sequenced. One set
105 consisted of 368 *H. brasiliensis* accessions, composed of both wild germplasm and cultivated
106 genotypes. Details of the plant materials can be found in de Souza *et al.* (2015) and Supplementary
107 Table 1. The other set is an important mapping population of the rubber tree consisting of 252 F1
108 hybrids, derived from a cross between PR255 x PB217 and comprising three replicates of each
109 parental genotype, which were mapped with 505 markers (SSRs, expressed sequence tag-SSRs, and
110 SNPs) prior to this publication (Souza *et al.*, 2013; Rosa *et al.*, submitted). Genomic DNA was
111 extracted from leaves using the DNeasy® Plant Mini Kit (QIAGEN, Germany) according to the
112 procedures described by the manufacturer. DNA quality parameters and concentrations were
113 measured using a UV-Vis spectrophotometer (NanoDrop, Thermo Scientific, Wilmington, DE, USA)
114 and agarose gels.

115 2.2 SNP discovery via GBS

116 GBS library preparation and sequencing were performed at the Institute of Genomic Diversity
117 (Cornell University, Ithaca, NY, USA) as described by Elshire *et al.* (2011). Genome complexity was
118 reduced by digesting individual genomic DNA samples with *EcoT22I*, a methylation-sensitive
119 restriction enzyme. The resultant fragments from each sample were directly ligated to a pair of
120 enzyme-specific adapters and combined into pools. PCR amplification was carried out to generate the
121 GBS libraries, which were sequenced on the Illumina HiSeq 2500 platform (Illumina Inc., USA). The
122 raw data were processed, and SNP calling was performed using TASSEL 5.0 (Glaubitz *et al.*, 2014).

123 Initially, the FASTQ files were demultiplexed according to the assigned barcode. The reads from
124 each sample were trimmed, and the tags were identified using the following parameters: Kmer length
125 of 64 bp, minimum quality score within the barcode and read length of 20, minimum Kmer length of
126 20. All sequence tags from each sample were aligned to the reference rubber tree genome (Tang *et*
127 *al.*, 2016) with Bowtie 2 (Langmead and Salzberg, 2012) using the very-sensitive option.

128 To perform the analysis, the data were divided into the mapping population and germplasms. SNP
129 calling was performed using the TASSEL 5 GBSv2 pipeline (Glaubitz *et al.*, 2014) and filtered using
130 VCFtools (Danecek *et al.*, 2011) with the following criteria: (1) missing data of 20%, (2) minor allele
131 frequency (MAF) greater than or equal to 5% (MAF 0.05), and (3) biallelic SNPs only.

132 **2.3 Genetic linkage map**

133 All linkage analyses were performed using OneMap software (Margarido *et al.*, 2007), version 2.0-1,
134 employing a previously constructed genetic map (Souza *et al.*, 2013; Rosa *et al.*, submitted) as a
135 basis for the inclusion of GBS-based SNPs with a minimum logarithm of odds (LOD) score of 8.21
136 (according to the function in the R package Onemap “suggest_lod”) and a maximum recombination
137 fraction of 0.35.

138 The map construction utilized only markers with 0.05 missing data and tested the pattern of allelic
139 segregation for χ^2 goodness of fit to the expected Mendelian segregation ratios, and markers with
140 significant segregation distortion were excluded from further analysis. GBS-based SNPs were added
141 to the previous genetic map using the ‘try.seq’ function in OneMap, which determines the best
142 position for a given unpositioned GBS marker in a specific linkage group (LG). Finally, the fractions
143 of recombination were converted to centimorgans (cM) using the Kosambi map function (Kosambi,
144 1943), and the map was drawn in Mapchart, version 2.3 (Voorrips, 2002).

145 **2.4 Population structure and genetic diversity**

146 The population structure was investigated in 368 genotypes from the germplasm collection with data
147 from SNPs anchored in a certain LG using two different methods: STRUCTURE analysis and
148 principal coordinate analysis (PCoA). Initially, the structure was analyzed with the software
149 STRUCTURE 2.3.4 (Pritchard *et al.*, 2000). Ten replications were run for each of the subpopulation
150 numbers (K), ranging from 1 to 10. Each run included 500,000 Markov chain Monte Carlo (MCMC)
151 iterations, among which the first 100,000 iterations (used to monitor whether a chain reached
152 stationarity) were discarded as burn-in. The delta K method was used to identify the number of
153 subgroups in the dataset (Evanno *et al.*, 2005). Based on the posterior probability of membership (Q)
154 of a given accession, the accession was classified as admixed in clusters with a membership of
155 Q<0.70. Subsequently, genetic distances between pairs of accessions were calculated, and PCoA was
156 performed for the SNPs using the GenAIEx program (version 6.5) (Peakall and Smouse, 2012).

157 **2.5 Analysis of LD**

158 LD was measured by calculating the squared correlation coefficient (r^2) between each pair of SNPs
159 with the R software and GGT 2.0 (van Berloo, 2008), using data from SNPs anchored in the genetic
160 map. We selected markers that were positioned on the linkage map and were present in the
161 germplasm to calculate the LD in each LG separately, considering the subgroup inferred with
162 STRUCTURE. The decay of LD over genetic distance was investigated by plotting pair-
163 wise r^2 values against the distance (cM) between markers on the same chromosome using the
164 following model: $y = a + be^{-c/x}$ (Ranc *et al.*, 2012), where x and y represent the genetic distance

165 in cM and the estimated r^2 , respectively. The critical r^2 for LD decay was determined by values of
166 0.1, which is considered the minimum threshold for a significant association between pairs of loci
167 and to describe the maximum genetic or physical distance at which LD is significant (Zhu *et al.*,
168 2008).

169 **3 Results**

170 **3.1 SNP discovery and evaluation**

171 The analysis was performed separately for the mapping population and germplasm to produce a total
172 of 1.785 million reads of sequence data, of which 89% (1,586 million reads) consisted of good
173 barcoded reads. Of these reads, 69,408 (23.42%) were aligned to the mapping population exactly one
174 time and 177,143 (59.78%) more than one time, corresponding to an 83.20% (246,551) overall
175 alignment rate. The total rate of alignment to the germplasm was 89.97% (818,807), of which
176 22.59% of the tags (205,576) were aligned to the rubber tree reference genome exactly one time
177 (Tang *et al.*, 2016) and 67.38% (613,231) more than one time.

178 A total of 386,180 SNPs were identified in the germplasm, and 76,191 SNPs were detected in the
179 mapping population, of which 350,965 SNPs (germplasm) and 66,453 SNPs (mapping population)
180 were biallelic. After excluding markers showing (1) more than 20% missing data or (2) a MAF \leq
181 0.05, the whole dataset was reduced to 77,660 and 21,283 SNPs in the germplasm and mapping
182 populations, respectively. The SNP frequencies were one biallelic SNP every 20.7 kb for the
183 mapping population and every 3.9 kb for the germplasm.

184 Sequence data are deposited under EMBL-EBI accession PRJEB26962.

185 **3.2 Saturation of the linkage map with SNPs**

186 From 21,283 SNPs, a total of 14,852 markers were selected after applying the chi-square test ($P \leq$
187 0.05), which revealed segregation ratios of 1:2:1 and 1:1. Markers exhibiting statistically significant
188 segregation distortion were excluded from further analysis to obtain accurate genetic linkage maps.
189 The data analyses were performed using SNPs with a maximum of 5% missing data, resulting in a
190 linkage map with 1,062 markers presenting 348 SSR markers (Souza *et al.*, 2013 and Mantello,
191 2014), 576 SNPs from GBS (Supplementary Table 2) and 138 SNPs markers genotyped using the
192 Sequenom MassARRAY® platform (AgenaBio, San Diego, CA) and the Fluidigm® platform (South
193 San Francisco, CA), developed from *de novo* transcriptome assemblies (Mantello *et al.*, 2014 and
194 Salgado *et al.*, 2014) and from EST full-length libraries (Silva *et al.*, 2014).

195 The genetic map was organized according to the numbers obtained from the map previously
196 developed by Rosa *et al.* (submitted). Eleven markers were removed after data diagnosis using heat
197 map graphs, thereby permitting the visualization of the recombination fraction and LOD scores from
198 markers, to group the SNPs in the LGs without changing the order of the base map. Only LG18 was
199 further divided into subgroups “A” and “B” (Figure 1).

200 Thus, a genetic map was generated spanning a cumulative length of 4,693 cM (Figure 1), distributed
201 among all the chromosomes. The LGs ranged from 23.8 cM (LG18B) (Supplementary Table 3) with
202 14 markers to the largest group with 404.6 cM (LG10) with 85 markers (of which 78 were from
203 GBS), and the average interval size between two adjacent markers was 4.4 cM.

204 The maximum gap size was 36.4 cM (LG11), which was maintained from the previous map.
205 Furthermore, some regions could not be sampled using the selected restriction enzyme; in LG16, for
206 example, only 2 GBS-based markers were added.

207 3.3 Genetic relationships among populations

208 The germplasm collection was selected in a prior work by Souza *et al.* (2015) examining the
209 population structure with SSR markers. To confirm the population structure of the sample of selected
210 individuals, we performed a new analysis as performed with the SNPs from GBS genotyping. Only
211 mapped SNPs that were common in the germplasm collection were used. Clustering inference
212 performed with K values ranging from 1 to 10 showed that the model likelihood increased steeply at
213 $K=2$, followed by a drastic decline starting at $K=3$, suggesting that the optimal K value was 2. The
214 assignment results for $K=2$ showed that some of the sampled individuals exhibited admixtures from
215 two gene pools (Figure 2(A)): group 1 (red bars) mainly consisted of accessions originating from the
216 Mato Grosso and cultivated genotypes, and group 2 (green bars) consisted entirely of wild accessions
217 from Amazonas, Rondônia, Para, and Acre (identified as IS - Ilha Solteira). Twenty-one accessions
218 showing a membership probability (Q value) below 0.70 were defined as admixed and were removed
219 from subsequent analyses.

220 As a second analysis of differentiation, we employed PCoA based on a similarity matrix that
221 explained 22.8% and 16.7% of the genetic variation with the first and second PCoA axes,
222 respectively. Plotting the two first PCoA axes separated the germplasm into two clusters, though
223 some overlap was present between the wild germplasms and cultivated genotypes (Figure 2). On the
224 first axis, most of the breeding genotypes were separated from the other genotypes. On the second
225 axis, the wild germplasm samples were clustered together, but some accessions from the Amazon
226 were isolated in their own subdivision.

227 3.4 Evaluation of LD

228 Based on population genetic structure, accessions could be divided into two distinct groups
229 (cultivated and wild group) (Figure 2), and pairwise LD estimates were performed within the gene
230 pool of each of these groups. To visualize LD throughout the genome, heat maps were produced
231 based on pairwise r^2 estimates, and corresponding p -values were calculated using permutations for all
232 marker pairs (Supplementary Figure 1). These heat maps were employed to identify variations in LD
233 between the cultivated and wild rubber tree germplasm groups.

234 In 16,025 pairwise combinations, we identified 186 (1.2%) and 592 (3.7%) statistically significant
235 associations that were in LD ($P<0.05$) in the cultivated and wild germplasms, respectively. Of these
236 significant associations, 78 and 64 were intrachromosomal in the cultivated and wild germplasms,
237 respectively, accounting for 0.5% and 0.4% of the total possible intrachromosomal correlations.
238 Among the unlinked loci, the proportions of LD were 0.7% and 3.3% for the cultivated and wild
239 germplasms, respectively. In both clusters, an uneven distribution of LD among the 18 chromosomes
240 was observed.

241 The strength of LD ($P<0.05$) was very different between two clusters, as reflected by the mean r^2
242 values of 0.49 and 0.02 obtained for the cultivated and wild germplasms, respectively. The 346 SNPs
243 that were localized in the integrated map were used for the estimation of LD decay among the
244 different LGs. LD decay was estimated across the germplasms and was found to be more pronounced
245 in the wild germplasms, with the range being dependent on the chromosome group (Supplementary
246 Figure 2). Using a fixed baseline r^2 value of 0.1 for the wild germplasm, LD decay ranged from 2.3

247 cM (LG9) to 11.4 cM (LG17). In contrast, in the cultivated accessions, this decay was slower,
248 ranging from 4.3 cM (LG8) to 50 cM (LG17), with average values of 5.6 cM and 19.6 cM for the
249 wild and cultivated germplasms, respectively (Figure 3). The patterns of LD can also be visualized
250 across the genome from the diagonal of the heat maps (Supplementary Figure 1).

251 **4 Discussion**

252 We performed a genetic mapping study with a bi-parental population (252 segregating hybrids
253 between PR255 x PB217) and analyzed the population structure and LD with two different
254 populations of rubber tree, formed from 47 accessions from a breeding program and 300 accessions
255 from a germplasm collection. For this study, we employed SNPs obtained via the GBS approach,
256 which enabled the detection of polymorphisms distributed across the genome.

257 An important breakthrough of the GBS approach is that a reference genome is not necessary for SNP
258 genotyping. However, the availability of a reference genome offers additional benefits, as it allows
259 proper alignment and ordering of the sequenced tags (Poland *et al.*, 2012). The first draft of the
260 genome sequence (Rahman *et al.*, 2013) provided a source of genomic information, after which
261 three more genomes were published (Tang *et al.*, 2016; Lau *et al.*, 2016; Pootakham *et al.*, 2017).
262 The assembly is highly fragmented, containing more than one million contigs. The assembly of a
263 complex genome is challenging, owing in part to the presence of highly repetitive DNA
264 sequences, which introduce ambiguity during genome reconstruction. We used the genome
265 published by Tang *et al.* (2016) to map the SNPs. The SNPs positioned on the map are named in
266 reference to the location of alignment with the genome.

267 Repetitive regions account for 71% of the *Hevea* genome (Tang *et al.*, 2016), posing a major
268 challenge for the *de novo* assembly, particularly when exclusively short-read data are used. This
269 phenomenon might explain the prevalence of tags that aligned to more than one unique region
270 (59.78% to the mapping population and 67.38% to the germplasm) (Tang *et al.*, 2016). Based on the
271 properties of the reference genome (characterized by a great accumulation of repetitive sequences,
272 primarily in heterochromatic regions) (Rahman *et al.*, 2013), the restriction enzyme *EcoT22I* was
273 selected because it is partially sensitive to methylation and rarely cuts retrotransposons.

274 The frequency of nucleotide substitutions was five times higher in the wild (3.9 kb) than in the
275 cultivated (20.7 kb) germplasm sequences. One explanation for this finding is that selection in
276 cultivated breeding programs acts to reduce diversity and alter allele frequencies in the DNA
277 sequence. Depending on how LD is increased surrounding these loci; the effects of such a selection
278 may not extend sufficiently far to affect the overall genome diversity. Rubber tree breeders have had
279 to develop cultivars that are appropriate for the specific temperature and humidity conditions
280 encountered in different cultivation areas, along with various biotic and abiotic stress resistance
281 factors. High-density SNPs are also common in non-genetic regions where there is no selection
282 pressure, and the abundance of these SNPs will be very useful for future assessments of breeding
283 populations. The high diversity of SNPs is characteristic of outbreeding trees; in other studies
284 examining rubber tree, Pootakham *et al.* (2011) previously identified a frequency of one SNP every
285 1.5 kb, while Pootakham *et al.* (2015) observed a frequency of one SNP every 308 nucleotides.

286 GBS does not require complete genome sequencing; only a targeted sequencing approach is
287 necessary. Due to its high-throughput efficiency, GBS has been used for SNP identification and
288 mapping in many plant species (Poland *et al.*, 2012; Rabbi *et al.*, 2014, Rimbert *et al.*, 2018, Bekele
289 *et al.* 2018). In rubber tree, most of the genetic linkage maps constructed to date have employed
290 molecular markers such as RFLPs and AFLPs (Lespinasse *et al.*, 2000) or microsatellites (SSRs) (Le
291 Guen *et al.*, 2011; Triwitayakorn *et al.*, 2011; Souza *et al.*, 2013). However, GBS was employed for

292 linkage map construction in rubber tree very recently (Pootakham *et al.*, 2015; Shearman *et al.*,
293 2015). In the present study, we utilized the GBS platform to sequence a PR255 x PB217 mapping
294 population that was previously saturated with SSR markers and SNPs obtained from other specific
295 platforms (Souza *et al.*, 2013; Rosa *et al.*, submitted).

296 The linkage map constructed in the present study exhibits a regular marker distribution. However, the
297 cumulative genetic map is significantly longer (4,693 cM) than would be expected for maps derived
298 from other mapping populations that have presented a lower resolution; for example, a map of 2,052
299 cM (Pootakham *et al.*, 2015) was obtained using only SNPs, and a map of 2,441 cM (Le Guen *et al.*,
300 2011) was obtained using both SSRs and AFLPs. Such expansions of the rubber tree genetic linkage
301 map have also reported previously (4,160 cM, Shearman *et al.*, 2015). Several factors may be
302 responsible for this phenomenon, including the numbers and types of mapped loci, the genetic
303 constitution of different mapping populations and differences in mapping strategies, the mapping
304 software and the ratio between the number of markers and the population size (Knox and Ellis,
305 2002).

306 Genetic mapping of the population (PR255 x PB217) was initiated in the first publication by Souza *et*
307 *al.* (2013) using microsatellite markers. These first LGs were organized according to the numbers
308 obtained from the map previously developed by Lespinasse *et al.* (2000), and information from other
309 maps (unpublished) consisting of microsatellites in common was used to identify syntenic markers.
310 Subsequently, the PR255 x PB217 mapping population was saturated with SSR markers and 243
311 SNPs obtained from platforms such as Sequenom MassARRAY iPLEX technology and KASP
312 genotyping (Rosa *et al.*, submitted). The SNPs from GBS used to construct the new genetic linkage
313 map contributed to reducing the average interval between two adjacent markers (4.4 cM versus 7.4
314 cM). However, the marker density remained lower than that of the first rubber tree map (Lespinasse
315 *et al.*, 2000), which presented one marker every 3 cM or 0.89 cM according to Pootakham *et al.*
316 (2015). LG11 displayed the maximum gap size (36.4 cM), which may have been caused by sections
317 of the genome that were identical among the parental genotypes and thus an absence of
318 polymorphisms, or by recombination hotspots. Large gaps exhibiting a low degree of polymorphisms
319 have also been reported by Shearman *et al.* (2015).

320 Genetic maps are important tools not only for QTL mapping but also for anchoring genome assembly
321 scaffolds into pseudo-chromosomes. The draft genome of *H. brasiliensis* has been reported to be
322 highly heterozygous, with 71% of the genome length comprising repeats (Tang *et al.*, 2016). A total
323 of 21,283 biallelic SNPs were identified, potentially aligning with 1,926 scaffolds, corresponding to
324 26% of the total scaffolds of the genome used. However, only 3% of these scaffolds were anchored to
325 LGs due to the relatively fragmented scaffold sequences and the usage of an insufficient genetic map
326 to anchor the scaffolds. Thus, it is important to develop higher-quality genetic maps to help improve
327 the scaffold anchoring ratio of future rubber tree genome assemblies.

328 Progress in the development of new molecular markers and genetic linkage maps is important for
329 genetic improvement in rubber tree breeding programs. Despite the economic and ecological
330 importance of this crop, restricted genomic resources are available for rubber tree. Sequencing of the
331 studied family allowed the identification and genotyping of many markers in an efficient and cost-
332 effective way. The linkage mapping analysis resulted in a number of LGs corresponding to the rubber
333 tree haploid chromosome number (n=18) (Ong, 1975; Lespinasse *et al.*, 2000), and the development
334 of GBS methods and genetic maps represents an important advancement of the genomics tools
335 available for these crops, which currently lack a good reference genome sequence.

336 Diversity analyses were performed in a previous work that included the entire collection of rubber
337 germplasm, analyzing 1,117 genotypes with 13 microsatellite markers (Souza *et al.*, 2015), and
338 showed a mean observed heterozygosity (H_o) of 0.64 and higher genetic diversity (H_e) than H_o in all
339 cases. Wright's fixation index (F) values were positive, with a mean of 0.16 obtained for the
340 accessions overall. Among a total of 408 observed alleles, 89 represented unique alleles to different
341 groups of accessions, demonstrating the high level of heterogeneity in these genotypes. To confirm
342 the population structure of the sample of selected individuals based on the work of de Souza *et al.*
343 (2015), a new analysis of the population structure was conducted with SNPs obtained from GBS
344 genotyping. The ΔK values obtained in this study indicated that the rubber tree germplasm could be
345 divided into two groups and showed that some of the sampled individuals exhibited admixtures from
346 two gene pools, which was also confirmed by plotting the two first PCoA axes.

347 Recent work using SSR markers has revealed similar results to those obtained using SNPs from GBS.
348 For example, Le Guen *et al.* (2009) demonstrated a separation between the Acre and Rondônia
349 groups and the Mato Grosso group. One possible reason for this separation is that the wild accessions
350 are from geographically distant populations that are not connected by hydrographic networks (Le
351 Guen *et al.*, 2009; Chanroj *et al.*, 2017), whereas most of the Wickham clones were collected from
352 regions that are geographically closer to the Mato Grosso and the Tapajós river, enabling rubber
353 seeds to flow from one region to another via the river. Souza *et al.* (2015) reported a difference in
354 genotypes between the two groups, which are in different river basins, thus separating the genotypes
355 in the cultivated and wild groups. Within the group of cultivated genotypes denoted as Mato Grosso
356 and Wickhan, genotypes collected from Mato Grosso were genetically close to genotypes used to
357 initiate the Asian breeding programs, denoted Wickhan genotypes in this article. These genotypes
358 were collected by Henry Wickhan in 1976 in the same basin from which the genotypes from Mato
359 Grosso were sampled (Gonçalves *et al.*, 1990). The results obtained by Souza *et al.* (2015)
360 corroborate the seminal study by Le Guen *et al.* (2009).

361 Population genetic structure is a principal factor influencing the generation of false positives and the
362 success of the association or LD mapping (Gupta *et al.*, 2005). These 368 rubber tree accessions
363 could be divided into two distinct groups based on population genetic structure: cultivated and wild
364 germplasm. The investigation of LD decay vs genetic distance based on markers is not possible
365 without prior information regarding the positions of markers in the genome. Since the information on
366 the rubber tree genome is still inaccurate regarding these positions, we employed the existing genetic
367 map of the PR255 x PB217 population to identify the positions of some SNPs and, thus, enable a
368 more accurate study of LD decay.

369 LD analysis with the mapped SNPs revealed that LD varied along the chromosomes, with regions of
370 high LD being interspersed with regions of low LD (Supplementary Figure 1). LD estimation is
371 possible without the positions of molecular markers along the genome and was indeed performed in
372 this study. However, these positions are crucial if one is interested in determining the decay or
373 extension of LD in relation to the genetic distance, regardless of by chromosome.

374 The average r^2 values were found to be very different when the two detected groups were compared.
375 This measurement was higher in the breeding germplasm (0.49) than in the wild germplasm (0.02),
376 corroborating the results of Chanroj *et al.* (2017), who suggested that these results were caused by
377 high gene flow in the wild Amazonian population. The breeding accessions exhibited a notably
378 higher level of LD, suggesting less genetic diversity in this subdivision, perhaps because of the
379 constraint of genetic variability employed in breeding programs due to the recurrent process of
380 selection. The low LD detected in the wild germplasm in this study was expected because perennial

381 outcrossing tree species display a high effective recombination rate, which leads to the rapid decay of
382 LD (Krutovsky and Neale, 2005).

383 The higher LD level detected in the cultivated group may have been influenced by the partly
384 identical-by-descent of these genotypes from a limited number of founders of the breeding programs,
385 with only a few generations between them. Thus, many longer pieces of chromosomes have not had
386 time to undergo disruptions. Domesticated crop cultivars necessarily represent a subset of the genetic
387 variation found in their wild ancestors, and the process of crop domestication is responsible for
388 genetic bottlenecks (McCouch, 2004). Although rubber tree breeding programs are very recent, the
389 differences in LD patterns detected between cultivated and wild germplasms suggest that plant
390 breeders may have selected for separate combinations of genes during the breeding process.
391 Moreover, selection for high latex yields and the extensive use of particular clones as parents in
392 rubber breeding programs have further reduced the genetic diversity of commercial rubber
393 germplasm (Priyadarshan, 2016), which may also affect LD.

394 LD decay was estimated at 25.7 cM within cultivated and 5.7 cM within wild germplasm, and
395 significant inter-chromosomal LD was identified within cultivated in contrast to wild germplasm.
396 The distances of LD decay between the two groups were most different in LGs 3, 5, 7, 10 and 11,
397 suggesting that these chromosomes may carry more genes related to agronomic traits that have been
398 selected via organized breeding of this crop. In previous studies involving Amazonian accessions of
399 rubber tree, Chanroj *et al.* (2017) revealed an LD decay of more than 0.5–6 cM and suggested that
400 LD estimates were significantly influenced by physical distance, with LD decay greater than 2 kbp
401 being observed in the widespread Amazonian population. These authors showed that LD decay over
402 genetic distance was different for the 18 different chromosomes, possibly because of the different
403 recombination rates of the 18 chromosomes. Rapid LD decay has been reported for many other
404 outcrossing tree species, such as *Populus nigra*, in which a decay of r^2 with distance in the *CAD4*
405 gene was observed at approximately 16 bp (Marroni *et al.*, 2011). In *Eucalyptus globulus*, candidate
406 genes for wood quality were analyzed using SNPs, and LD was estimated to decay rapidly
407 (Thavamanikumar *et al.*, 2011). Most LD estimation studies conducted in tree species are based on
408 candidate genes (Krutovsky and Neale, 2005).

409 LD mapping relies on germplasm samples and, as such, does not require the development of
410 experimental crosses with specific genetic backgrounds, and thus ease of use is an obvious benefit in
411 studies of perennial species with long life cycles. LD is a key factor in determining the number of
412 markers needed for genome-wide association studies (GWAS) and genomic selection (GS). Genomes
413 with low LD require a high marker density for GWAS or GS; therefore, our SNPs may be valuable
414 for GWAS in rubber tree breeding. Considering the length of the genetic map (4,693 cM) and the
415 mean LD observed (0.49 in breeding and 0.02 in wild populations), many evenly spaced SNPs would
416 be necessary to perform GWAS in the rubber tree, and the wilder the genotypes that are used, the
417 more difficult is the saturation of the mapping. However, to obtain a sufficient SNP density
418 throughout the genome and to account for variation in LD along the chromosomes more markers
419 must be genotyped. Our study results provide a valuable resource for further genetic studies
420 involving linkage or association mapping, marker-assisted breeding and *Hevea* sequence assembly
421 and comparative mapping.

422 Furthermore, GWAS of wild germplasm accessions in the future will provide a substantial
423 contribution to dealing with new challenging situations that will arise as a consequence of global
424 climatic changes. Useful QTLs and genes to face these new situations are currently unknown, but the
425 best way to identify them would be through analyses relying on GWAS of large panels of wild

426 genotypes. A precise assessment of the LD pattern across the genome of *Hevea* is necessary for such
427 endeavors, and the present study supplies a major contribution to this goal.

428 **Conflict of interest**

429 The authors have no conflicts of interest to declare.

430 **Author contributions**

431 LMS, LHS, VG and AS designed the study and performed the experiments; LMS, LHS, AC, CS,
432 CM, EJ, JF, and MM performed the experiments; LMS, LHS, JR, GM, VG, MM, PG and AG
433 analyzed the data; and LMS, LHS and AS wrote the manuscript.

434 **Funding**

435 The authors gratefully acknowledge the Fundação de Amparo a Pesquisa do Estado de São Paulo
436 (FAPESP) (2007/50392-1; 2012/50491-8) for financial support and for graduate scholarships to CM
437 (2011/50188-0, 2014/18755-0) and CS (2009/52975-0) and LHS (2014/11807-5, 2017/07908-9) and
438 a post-doctoral fellowship to LMS (2012/05473-1); the Conselho Nacional de Desenvolvimento
439 Científico e Tecnológico (CNPq) for financial support (478701/2012-8; 402954/2012-2), a post-
440 doctoral fellowship to CS, and research fellowships to AG, AS and PG and, a PhD fellowship to AC;
441 and the Coordenação de Aperfeiçoamento do Pessoal de Nível Superior (CAPES) for financial
442 support (Computational Biology Program and CAPES-Agropolis Program) and post-doctoral
443 fellowships to LMS and AC.

444 **References**

445 Bekele, W. A., Wight, C. P., Chao, S., Howarth, C. J. and Tinker, N. A. (2018), Haplotype based
446 genotyping-by-sequencing in oat genome research. *Plant Biotechnol. J.* Accepted Author
447 Manuscript. doi:10.1111/pbi.12888

448 Chanroj, V., Rattanawong, R., Phumichai, T., Tangphatsornruang, S., and Ukoskit, K. (2017).
449 Genome-wide association mapping of latex yield and girth in Amazonian accessions of *Hevea*
450 *brasiliensis* grown in a suboptimal climate zone. *Genomics* 109, 475-484. doi:
451 10.1016/j.ygeno.2017.1007.1005

452 Danecek, P., Auton, A., Abecasis, G., Albers, C.A., Banks, E., DePristo, M.A., et al. (2011). The
453 variant call format and VCFtools. *Bioinformatics* 27, 2156-2158.

454 de Souza, L.M., Le Guen, V., Cerqueira-Silva, C.B.M., Silva, C.C., Mantello, C.C., Conson, A.R.O.,
455 et al. (2015). Genetic diversity strategy for the management and use of rubber genetic
456 resources: more than 1,000 wild and cultivated accessions in a 100-genotype core collection.
457 *PLoS One* 10, e0134607.

458 Elshire, R.J., Glaubitz, J.C., Sun, Q., Poland, J.A., Kawamoto, K., Buckler, E.S., et al. (2011). A
459 robust, simple genotyping-by-sequencing (GBS) approach for high diversity species. *PLoS*
460 *One* 6, e19379.

461 Evanno, G., Regnaut, S., and Goudet, J. (2005). Detecting the number of clusters of individuals using
462 the software STRUCTURE: a simulation study. *Mol. Ecol.* 14, 2611–2620. doi:
463 10.1111/j.1365-294X.2005.02553.x

464 Glaubitz, J.C., Casstevens, T.M., Lu, F., Harriman, J., Elshire, R.J., Sun, Q., et al. (2014). TASSEL-
465 GBS: a high capacity genotyping by sequencing analysis pipeline. *PLoS One* 9, e90346.

466 Gonçalves, P.S., Cardoso, M., Ortolani, A.A. (1990). Origem, variabilidade e domesticação da
467 Hevea: uma revisão. *Pesquisa agropecuária brasileira* 25, 135-156.

468 Gupta, P.K., Rustgi, S., and Kulwal, P.L. (2005). Linkage disequilibrium and association studies in
469 higher plants: present status and future prospects. *Plant Mol. Biol.* 57, 461-485.

470 Knox, M.R., Ellis, T.H.N. (2002). Excess heterozygosity contributes to genetic map expansion in pea
471 recombinant inbred populations. *Genetics* 162, 861-873.

472 Kosambi, D.D. (1943). The estimation of map distances from recombination values. *Ann. Eugen.* 12,
473 172-175.

474 Krutovsky, K.V., and Neale, D.B. (2005). Nucleotide diversity and linkage disequilibrium in cold-
475 hardiness- and wood quality-related candidate genes in Douglas fir. *Genetics* 171, 2029-2041.

476 Langmead, B., and Salzberg, S.L. (2012). Fast gapped-read alignment with Bowtie 2. *Nat. Methods*
477 9, 357-359.

478 Lau, N.-S.; Makita, Y.; Kawashima, M.; Taylor, T.D.; Kondo, S.; Othman, A.S.; Shu-Chien, A.C.;
479 Matsui, M. The rubber tree genome shows expansion of gene family associated with rubber
480 biosynthesis. *Sci. Rep.* 2016, 6, 28594. doi: 10.1038/srep28594 (2016).

481 Le Guen, V., Doaré, F., Weber, C., and Seguin, M. (2009). Genetic structure of Amazonian
482 populations of *Hevea brasiliensis* is shaped by hydrographical network and isolation by
483 distance. *Tree Genet. Genomes* 5, 673-683.

484 Le Guen, V., Garcia, D., Doaré, F., Mattos, C.R.R., Condina, V., Couturier, C., et al. (2011). A
485 rubber tree's durable resistance to *Microcyclus ulmi* is conferred by a qualitative gene and a
486 major quantitative resistance factor. *Tree Genet. Genomes* 7, 877-889.

487 Lespinasse, D., Rodier-Goud, M., Grivet, L., Leconte, A., Legnate, H., and Seguin, M. (2000). A
488 saturated genetic linkage map of rubber tree (*Hevea* spp.) based on RFLP, AFLP,
489 microsatellite, and isozyme markers. *Theor. Appl. Genet.* 100, 127-138.

490 Mantello C.C., Cardoso-Silva C.B., da Silva C.C., de Souza L.M., Scaloppi Junior E.J., de Souza
491 G.P., et al. (2014). De novo assembly and transcriptome analysis of the rubber tree (*Hevea*
492 *brasiliensis*) and SNP markers development for rubber biosynthesis pathways. *PLoS One* 9,
493 e102665.

494 Mantello, C.C. (2014). Mapeamento genético molecular em *Hevea brasiliensis*. PhD Thesis:
495 Universidade Estadual de Campinas.

496 Margarido, G.R., Souza, A.P., and Garcia, A.A. (2007). OneMap: software for genetic mapping in
497 outcrossing species. *Hereditas* 144, 78-79.

498 Marroni, F., Pinosio, S., Zaina, G., Fogolari, F., Felice, N., Cattonaro, F., et al. (2011). Nucleotide
499 diversity and linkage disequilibrium in *Populus nigra* cinnamyl alcohol dehydrogenase
500 CAD4 gene. *Tree Genet. Genomes* 7, 1011-1023.

501 McCouch, S. (2004). Diversifying selection in plant breeding. *PLoS Biol.* 2, e347.

502 Ong, S.H. (1975) Citology of *Hevea*. In: RRIM Short Course in *Hevea* breeding. Kuala Lumpur:
503 RRIM, 21p.

504 Peakall, R., and Smouse, P.E. (2012). GenAlEx 6.5: genetic analysis in Excel. Population genetic
505 software for teaching and research—an update. *Bioinformatics* 28, 2537-2539.

506 Poland, J.A., Brown, P.J., Sorrells, M.E., and Jannink, J.L. (2012). Development of high-density
507 genetic maps for barley and wheat using a novel two-enzyme genotyping-by-sequencing
508 approach. *PLoS One* 7, e32253.

509 Pootakham, W., Chanprasert, J., Jomchai, N., Sangsrakru, D., Yoocha, T., Therawattanasuk, K., et al.
510 (2011). Single nucleotide polymorphism marker development in the rubber tree, *Hevea*
511 *brasiliensis* (Euphorbiaceae). *Am. J. Bot.* 98, e337-e338.

512 Pootakham W, Sonthirod C, Naktang C, Ruang-Areerate P, Yoocha T, Sangsrakru D,
513 Theerawattanasuk K, Rattanawong R, Lekawipat N, Tangphatsornruang S. De novo hybrid
514 assembly of the rubber tree genome reveals evidence of paleotetraploidy in *Hevea* species.
515 *Sci Rep.* 2017;7:41457.

516 Pootakham, W., Ruang-Areerate, P., Jomchai, N., Sonthirod, C., Sangsrakru, D., Yoocha, T., et al.
517 (2015). Construction of a high-density integrated genetic linkage map of rubber tree (*Hevea*
518 *brasiliensis*) using genotyping-by-sequencing (GBS). *Front. Plant Sci.* 6, 367.

519 Pritchard, J.K., Stephens, M., and Donnelly, P. (2000). Inference of population structure using
520 multilocus genotype data. *Genetics* 155, 945-959.

521 Priyadarshan, P.M. (2016). “Genetic diversity and erosion in *Hevea* rubber,” in *Genetic Diversity and*
522 *Erosion in Plants: Case Histories*, eds. M.R. Ahuja and S.M. Jain (Cham: Springer
523 International Publishing), 233-267.

524 Priyadarshan, P.M., and Goncalves, P.S. (2003). *Hevea* gene pool for breeding. *Genet. Resour. Crop*
525 *Evol.* 50, 101-114.

526 Rabbi IY, Hamblin MT, Kumar PL, Gedil MA, Ikpan AS, Jannink JL, et al. (2014). High-resolution
527 mapping of resistance to cassava mosaic geminiviruses in cassava using genotyping-by-
528 sequencing and its implications for breeding. *Virus Res.* 186:87–96.

529 Rahman, A.Y., Usharraj, A.O., Misra, B.B., Thottathil, G.P., Jayasekaran, K., Feng, Y., et al. (2013).
530 Draft genome sequence of the rubber tree *Hevea brasiliensis*. *BMC Genomics* 14, 75.

531 Ranc, N., Muños, S., Xu, J., Le Paslier, M.C., Chauveau, A., Bounon, R., et al. (2012). Genome-wide
532 association mapping in tomato (*Solanum lycopersicum*) is possible using genome admixture
533 of *Solanum lycopersicum* var. cerasiforme. *G3* 2, 853-864.

534 Rimbert, H., Darrier, B., Navarro, J., Kitt, J., Choulet, F., Leveugle, M., et al. (2018) High
535 throughput SNP discovery and genotyping in hexaploid wheat. *PLoS ONE* 13, e0186329.
536 <https://doi.org/10.1371/journal.pone.0186329>

537 Rosa, J.R.B., Mantello, C.C., Garcia, D., Souza, L.M., Silva, C.C., Gazaffi, R., et al. QTL detection
538 for growth and latex production in a full-sib population of rubber tree cultivated under
539 suboptimal climate conditions. Submitted.

540 Salgado L., Koop D., Pinheiro D., Rivallan R., Le Guen V., Nicolas M., de Almeida L.G., Rocha V.,
541 Magalhaes M., Gerber A. et al (2014): De novo transcriptome analysis of *Hevea brasiliensis*
542 tissues by RNA-seq and screening for molecular markers. *BMC Genomics* 15, 236.

543 Shearman, J.R., Sangsrakru, D., Jomchai, N., Ruang-Areerate, P., Sonthirod, C., Naktang, C., et al.
544 (2015). SNP identification from RNA sequencing and linkage map construction of rubber tree
545 for anchoring the draft genome. *PLoS One* 10, e0121961.

546 Silva C.C., Mantello C.C., Campos T., Souza L.M., Gonçalves P.S., Souza A.P. (2014) Leaf-, panel-
547 and latex-expressed sequenced tags from the rubber tree (*Hevea brasiliensis*) under cold-
548 stressed and suboptimal growing conditions: the development of gene-targeted functional
549 markers for stress response. *Molecular Breeding* 34, 1035-1053.

550 Souza, L.M., Gazaffi, R., Mantello, C.C., Silva, C.C., Garcia, D., Le Guen, V., et al. (2013). QTL
551 mapping of growth-related traits in a full-sib family of rubber tree (*Hevea brasiliensis*)
552 evaluated in a sub-tropical climate. *PLoS One* 8, e61238.

553 Tang, C., Yang, M., Fang, Y., Luo, Y., Gao, S., Xiao, X., et al. (2016). The rubber tree genome
554 reveals new insights into rubber production and species adaptation. *Nat. Plants* 2, 16073.

555 Thavamanikumar, S., McManus, L.J., Tibbits, J.F.G., and Bossinger, G. (2011). The significance of
556 single nucleotide polymorphisms (SNPs) in *Eucalyptus globulus* breeding programs. *Aust.*
557 *For.* 74, 23-29.

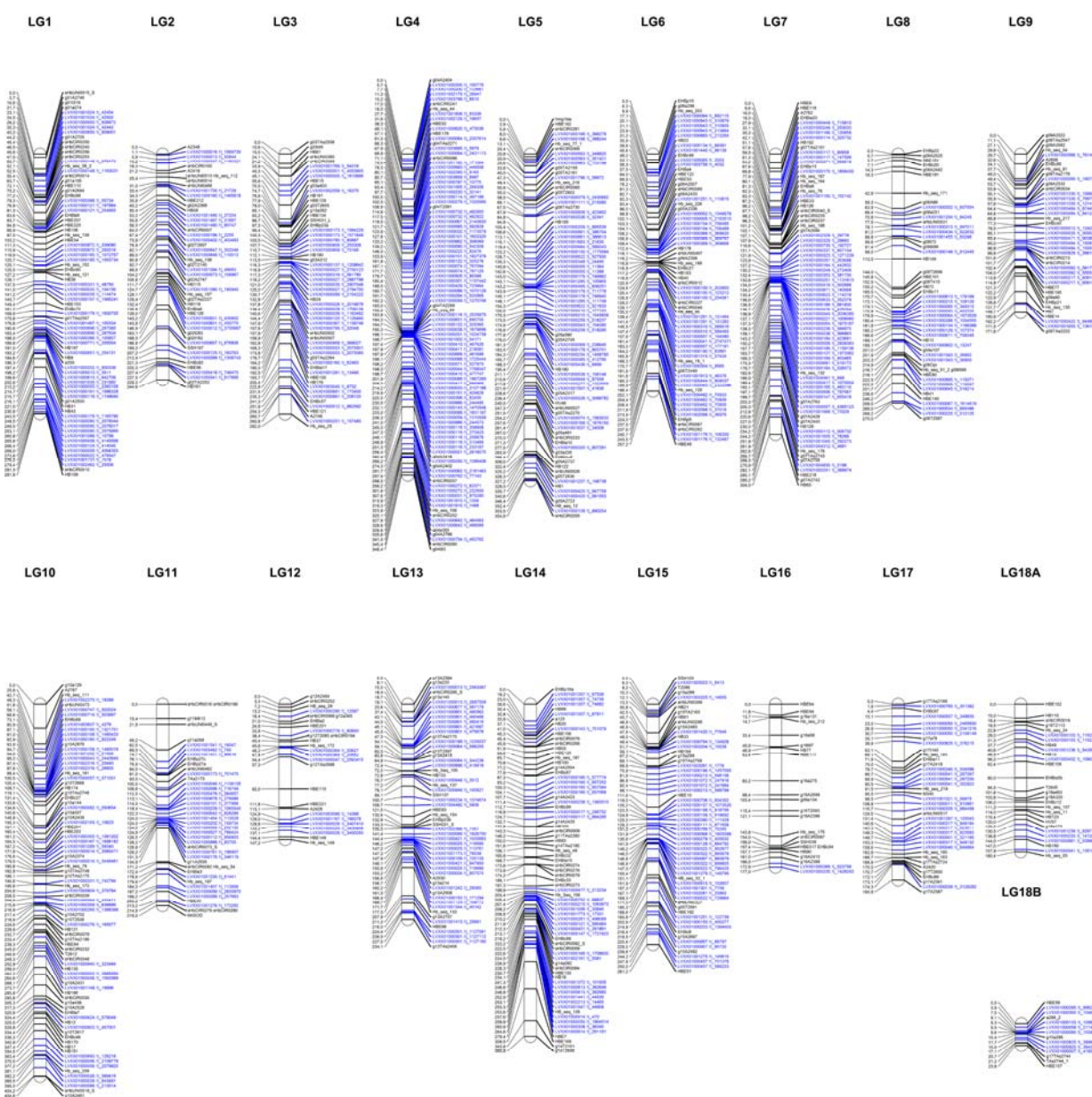
558 Triwitayakorn, K., Chatkulkawin, P., Kanjanawattanawong, S., Sraphet, S., Yoocha, T., Sangsrakru,
559 D., et al. (2011). Transcriptome sequencing of *Hevea brasiliensis* for development of
560 microsatellite markers and construction of a genetic linkage map. *DNA Res.* 18, 471-482.

561 van Berloo, R. (2008). GGT 2.0: versatile software for visualization and analysis of genetic data. *J.*
562 *Hered.* 99, 232-236.

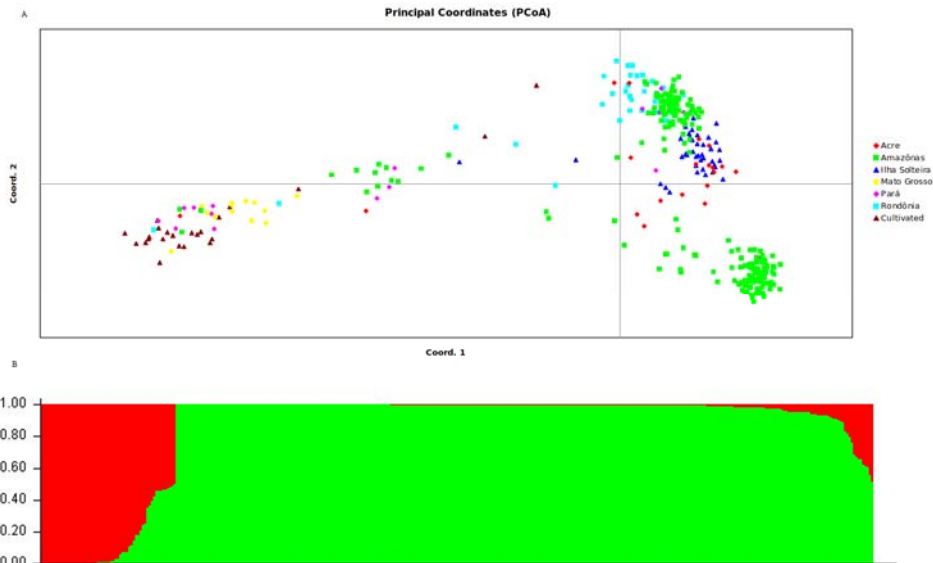
563 Voorrips, R.E. (2002). MapChart: software for the graphical presentation of linkage maps and QTLs.
564 *J. Hered.* 93, 77-78.

565 Weir, B.S. (1979). Inferences about linkage disequilibrium. *Biometrics* 35, 235-254.

566 Zhu, C., Gore, M., Buckler, E.S., and Yu, J. (2008). Status and prospects of association mapping in
567 plants. *Plant Genome* 1, 5–20.

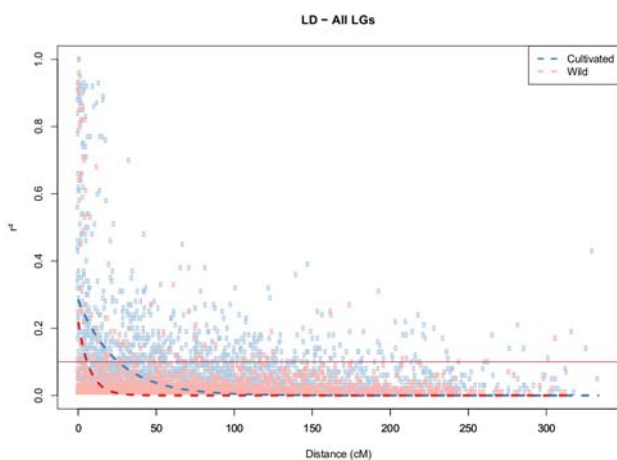


569 **Figure 1.** Linkage map of the rubber tree. Markers in blue represent SNPs obtained using the
570 genotyping-by-sequencing technique, and markers in black were obtained from the previous map
571 (Rosa *et al.*, SUBMITTED).



572

573 **Figure 2.** Estimated genetic structure of the wild population and breeding population of rubber tree
574 based on PCoA (A) and STRUCTURE analysis (B). All analyses are based on the genetic variability
575 of 438 SNP loci.



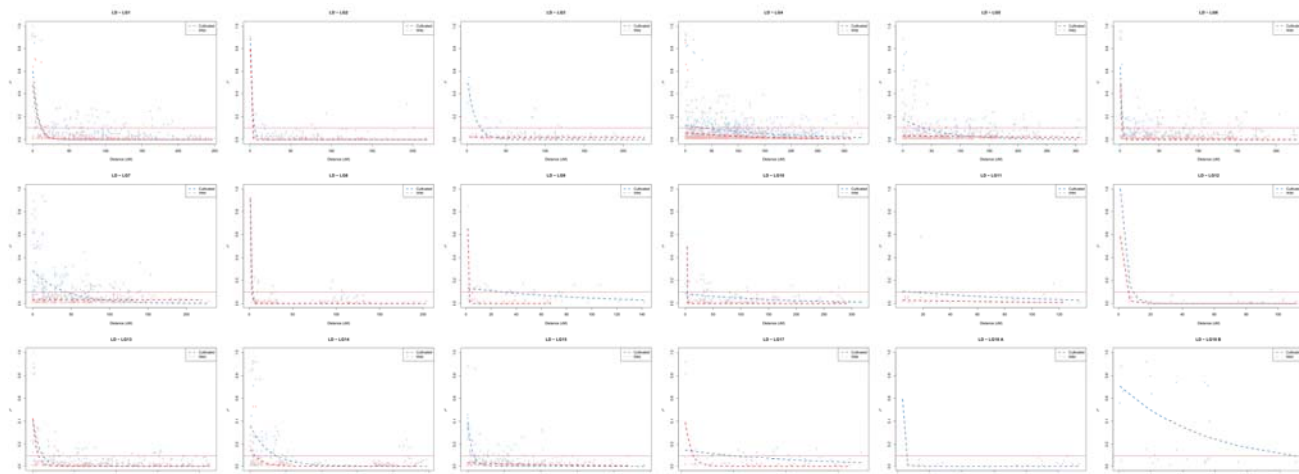
576

577 **Figure 3.** Decay of LD (r^2) as a function of genetic distance (cM) between pairs of loci on all
578 chromosomes. Only r^2 values with $P < 0.05$ are shown.



579

580 **Supplementary Figure 1.** Plots of LD heat maps for (A) with 47 breeding accessions and (B) with
581 300 accessions from wild germplasms. The rubber tree LGs are represented by a diagonal bar.
582 Markers were ordered on the x- and y-axes based on genomic location; therefore, each cell of the
583 heat map represents a single marker pair. The r^2 values for each marker pair are presented in the
584 bottom half of the heat map and are represented by shades of red increasing in intensity in equal
585 increments of 0.1 from 0.0 (white) to 1.0 (red).



586

587 **Supplementary Figure 2.** Decay of LD (r^2) as a function of genetic distance (cM) between pairs of
588 loci in individual LGs. Only r^2 values with $P < 0.05$ are shown.

589 Tables legends

590 **Supplementary Table 1.** Origin of germplasm genotypes and population structure results.

591 **Supplementary Table 2** SNPs from GBS and their genome information. The name of markers are in
592 agreement with the sequences of the reference genome (Tang *et al.*, 2016).

593 **Supplementary Table 3.** Marker information for the genetic map.

594